RESEARCH ARTICLE

A Pseudo Random Pursuit Strategy for Atomic Clocks

QIAN XU[1], YU CHEN[2], YUZHUO WANG[1], YUAN GAO[1], AND AIMIN ZHANG[1]
[1]National Institute of Metrology, Beijing 100029, China
[2]China National Intellectual Property Administration, Beijing 100088, China

Corresponding author: Yuzhuo Wang (wangyzh@nim.ac.cn)

ABSTRACT The atomic clock prediction algorithm is a critical part of the atomic time scale system to ensure its stability and accuracy. Random pursuit strategy (RPS) has been verified on the prediction capability of hydrogen maser and cesium clock in our previous works. This method is applied to deal with data impacted by different noise types including hetero-variance white noises and jumps. Nevertheless, it is difficult to apply RPS to real-time clock prediction, owing to its computational complexity. To alleviate it, we further improved our original algorithm by simplifying the random grouping using a pseudo-random strategy. In our work, theoretical analysis and necessary simulations of the pseudo-random pursuit strategy (PRPS) are presented, and the experimental results show PRPS's remarkable advantage in terms of operational efficiency. Compared to the original algorithm, it shows comparable accuracy and stability for prediction. PRPS takes only *1/p* fitting time consumption as long as RPS starts from the second prediction. PRPS is faster, more efficient, and easier to employ when utilizing a clock predictor as the output of a system than RPS.

INDEX TERMS Atomic clock, pseudo random, real-time prediction, anomalous behaviors, uncertainty, time complexity.

I. INTRODUCTION

As an important basic physical quantity, time plays an increasingly significant role in basic scientific research. It generally originates from a time scale mainly consisting of an atomic clock [1], [2], [3]. For instance, Coordinated Universal Time (UTC), which is produced by the International Bureau of Weights and Measures (BIPM), is derived from readings taken from about 450 free-running atomic clocks that are dispersed across the globe in more than 80 time laboratories [3], [4]. Most national metrology institutes (NMIs) maintain a relatively independent physical time scale system UTC(k), a realization of UTC. Based on a widely accepted view 'a good clock is a predictable clock' [3], [5], [6], predictability is the key to evaluating the performance of the atomic clock and it determines partly the accuracy and stability of the time scale. The positioning and navigating

The associate editor coordinating the review of this manuscript and approving it for publication was Cesar Vargas-Rosales.

capability of the global navigation satellite system (GNSS) depend primarily on the accurate time provided by atomic clocks [7], [8], [9], [10], [11], [12]. Under these cases, the anomalous clock behaviors [13], [14], [15], such as frequency jumps and frequency drift jumps, would have a serious impact on the overall performance of the time scale [1], [16], [17].

Many papers on atomic clock prediction have been reported in recent years. A mathematical model method based on stochastic differential equations was proposed for clock prediction [18], [19]. Preparing a better dataset of time series for prediction [20] and proposing a new way to generate UTC(PTB) which is the local time scale of Physikalisch-Technische Bundesanstalt (PTB) with a virtual clock [21] are also efficient. The majority of research, however, concentrated on identifying and reducing the impact of anomalous behaviors on atomic clock prediction [22], [23], [24], [25]. The random variation in the output frequency signal of atomic clocks is generally described with a nonstationary power-law spectrum noise model. White frequency noise (WFN) and

random walk frequency noise are primarily the dominating noises of the cesium clock and hydrogen maser (RWFN) [26]. Based on this perspective, stochastic differential equations [13], [26], [27], the optimal strategy, and the two-state theoretical model were used to deal with the non-stationary behaviors of atomic clocks [28] and to accurately estimate their phase, frequency, and frequency drift to improve their ability to keep accurate time. A problem still exists in improving atomic clock predictability and minimizing the effects of aberrant clock behavior.

As in the previous research, the random pursuit strategy (RPS) was used to reduce the influence of anomalous clock behaviors on its predictability [29], [30]. It was derived from Bagging [31], [32], which is a classical method of combinatorial optimization theory. The RPS was an ensemble prediction approach made up of some predictors, and each predictor was applied using sampling without replacement to a subset of the original sample data set. Ma et al. [33] has demonstrated that the parameters' values of each predictor estimated for all data via random sampling are unbiased estimates of true parameters' values, whereas also conditional unbiased estimates of parameters' values by ordinary least squares (OLS) of all samples. Utilizing a weighted average, the final forecast aggregated the results of the individual predictors. Based on the original RPS algorithm, an improved algorithm, the pseudo random pursuit strategy (PRPS), is designed to enhance its operating efficiency. It only performs the polynomial fitting operation for a subset including updated sample data via the moving windows. As a result, the amount of fitting operation times are greatly reduced, which enhances the efficiency of the proposed algorithm.

Although there is a tolerable efficiency for the post-processing prediction by RPS, such as UTC, the computation cost due to the random grouping and polynomial fitting in each subset is still a barrier in the real-time physical time scale system application, such as UTC(k) and GNSS. The proposed PRPS makes it easier to implement these real-time prediction tasks and could reduce the hardware cost at the same time.

II. PREDICTION ALGORITHM

For atomic clock data processing, the common technique are low-order polynomial [6], [17] methods and methods based on the Kalman filter [34], [35], [36], [37]. The low-order polynomial approach is simple and directly from the mathematical theory model of the atomic clock. For least square (LS) fitting or regression, the pre-condition or assumption for the noise is independent identical distribution and according to the central limit Theory, the residuals should be a normal distribution and the fitting operation always tends to make the residuals conform to a normal distribution. This is the same reason why the LS fitting is sensitive to jumps, because jumps do not satisfy noisy assumptions of fitting, and to fit them, parameters of a low-order polynomial are biased and have to be modified so that the normal distribution

to which residuals correspond has larger variance than the corrected situation. On the other hand, the Kalman filter approach requires more prior knowledge of the noise for update and prediction steps, and there are challenges for practical use in the selection of parameters' initializing values and a change of noise characteristics introduced by anomalous behaviors. As a result, the RPS or PRPS is proposed to deal with the clock data prediction influenced by anomalous behaviors, especially for which perturb only a single (or a few sparsely distributed) reading(s) in the time series. Although the robust least square fitting or the median filter is a common method to deal with jumps, we emphasize that RPS can handle multiple forms of anomalous behaviors including minor jumps [29]. The robust least square fitting or median filter is not helpful for minor jumps. In other words, our method is applied to deal with data impacted by different noise types including hetero-variance white noises and jumps.

A. PRPS

As shown in Fig.1, the RPS flowchart is represented and six steps were constructed to accomplish an ensemble prediction [38]. The RPS significantly improves the robustness of the prediction system by reducing the influence of jumps because corresponding predictors are assigned smaller weights, compared with the others. The design of the random grouping guarantees that anomalous behaviors are assigned to different predictors as much as possible and the design of ensemble predictors makes the effect of jumps weakened. It is clear the former design is suitable for continuous jumps, multiple jumps, and even missing data in a sample data vector and the latter design is a means to suppress the impact of jumps.

The RPS can be performed using any sample data vector, whether continuous prediction or non-continuous prediction is applied. However, when the prediction situation is simplified to a continuous one and there are no missing samples in clock data, the random grouping could be instead of an index adjustment in the PRPS flowchart step (2) in Fig.1. As a consequence, only one-time polynomial fitting is applied to an updated subset in the next time step.

The details of the PRPS are introduced below.

As shown in Fig.1, the prediction process of the PRPS for the first time is consistent with RPS, which includes several steps:

(1) In a timekeeping laboratory, the difference in time or frequency between an atomic clock and its reference at time interval T is directly monitored.

$$D = \{d_{t-n+1}, d_{t-n+2}, \ldots d_t\} \tag{1}$$

where D denotes a sample data vector derived from the measured values and d_t, t denotes one measured value at the t-th period time. By choosing an adequate data length n, D could generally replicate the characteristics of the atomic clock disturbances as closely as reasonable.

(2) Randomly divide n original data in D into p subsets, and each subset contains m measured values. The selection of p and m will have a slight impact on the final results.
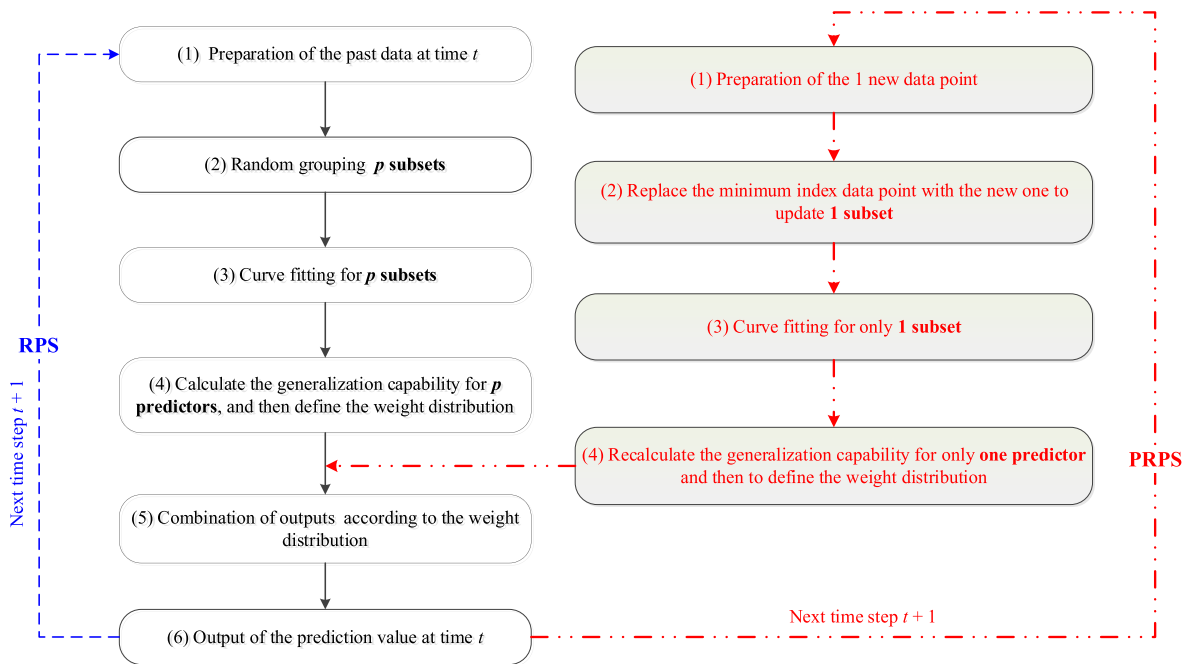
FIGURE 1. Comparison between the RPS and PRPS.

The strategy $p = m = \sqrt{n}$ is proposed to select the two parameters.

(3) The least square approach is used to perform fitting and obtain $f_j(t, A_j)$ since each subset is treated independently as a separate previous data group, where t and A_j are the epoch and parameter vectors of fitting, respectively. A typically consists of phase, frequency, and frequency drift on a physical level. The predictor ensemble is made up of the functions produced from p subsets.

(4) Each $f_j(t, A_j)$'s ability to predict can be characterized in terms of particular interests. Our previous work [30] described the calculation method of the uncertainty of predicted value $\hat{d}_j(t)$ in detail. It is defined as a generalization capability of $f_j(t, A_j)$ in this work, therefore the weight of that in the ensemble can be expressed as

$$\omega_j = \frac{1}{u^2_{\hat{d}_j(t)}} / \sum_{j=1}^{p} \frac{1}{u^2_{\hat{d}_j(t)}} \qquad (2)$$

The $u^2_{\hat{d}_j(t)}$ is the sum of squared residuals, $\hat{d}_j(t)$ is fitted based on the j-th subset of measured values.

(5) The future data d_{t+1} is predicted by the weighted average of the predictor ensemble. Therefore, the prediction value $\hat{d}_{t+1}$ can be expressed as:

$$\hat{d}(t+1) = \sum_{j=1}^{p} \omega_j \cdot \hat{d}_j(t+1) \qquad (3)$$

If the prediction value $\hat{d}_j(t)$ from subset j is a posterior distribution, the value $\hat{d}(t+1)$ acts as a weighted average of all the posterior distributions.

(6) At last, the procedure outputs the prediction value $\hat{d}(t+1)$ at time $t+1$.

For the next prediction in Fig.1, the PRPS no longer performs random grouping like RPS but a pseudo random strategy was designed to enhance its operational efficiency. Supposing the data d_i with the minimum index i in the subset j, it is replaced with the new measured value at time $t+1$. Thus, only the predictor j needs to perform a polynomial fitting again to obtain the new predicted value. Compared to RPS, it saves computation costs in random grouping and polynomial fitting for p-1 subsets. In other words, if RPS takes t to make a prediction, it takes only t/p to make a prediction by the PRPS. Obviously, the PRPS improves by an order of magnitude in operation efficiency. In section III, we will further investigate the difference between the operation efficiency and atomic clock predictability between the RPS and PRPS.

B. ONE EMBODIMENT OF THE PRPS

In general, three parameters—phase, frequency, and frequency drift—can be used to describe the readings of Cs-clocks and H-masers [29], [30] about the modified Julian date (MJD). The prediction of the clock phase is the main emphasis of this example. The way it is written as:

$$f_j(t, A_j) = a_j + b_j t + c_j t^2 \qquad (4)$$

where t is the epoch, and $f_j(t, A_j)$ represents the predictor j's prediction value, $A_j = \{a_j, b_j, c_j\}$, a_j, b_j and c_j is the estimated value of the jth predictor's phase, frequency, and frequency drift. This clock's forty-nine historical data points numbered one through forty-nine, were divided into seven subgroups at random (n = 49). The first prediction in table 1 includes a list

TABLE 1. A randomized grouping.

Subset	Random sample	Parameters (a_j, b_j, c_j)	Weight	Prediction value f_j
	1st prediction			
1	48 47 38 20 2 40 46	-1.0799, 0.4595, -0.0104	0.13	-4.19
2	12 43 15 28 41 26 49	-6.2383, 0.6621, -0.0122	0.12	-3.66
3	18 33 16 23 32 37 3	-1.2125, 0.3052, -0.0051	0.09	1.21
4	4 10 45 17 24 27 13	-3.0427, 0.4366, -0.0090	0.19	-3.79
5	25 42 35 14 29 1 39	-0.5952, 0.2701, -0.0055	0.15	-0.99
6	5 36 44 8 30 7 9	-5.0495, 0.6602, -0.0127	0.20	-3.89
7	19 31 6 22 21 11 34	-4.9704, 0.6350, -0.0112	0.12	-1.37
	2nd prediction			
5	25 42 35 14 29 50 39	-7.5022, 0.7863, -0.0143	0.12	-4.67

of one randomized group. The following point f_j ($t = 50$) can be derived using the weighted average of the seven predictors. The detailed procedure of calculation is discussed in part A of section II. Different from RPS, starting from the second predicted point f_j ($t = 51$), in the PRPS, a new incoming point would replace the earliest point and a new polynomial fitting replaced the original one. For instance, in the 2nd prediction in table 1, the new incoming point number 50 is updated for the 5th subset due to the earliest point numbered 1 being removed, and the next step of PRPS is fitting a polynomial of the 5th subset only, and updating the weight. Although only one point gets replaced as the sampling window moves, all other subset weights are also changed due to the $u^2_{\hat{d}_j(t)}$ being the sum of squared residuals about the new sampling window. In other words, each $u^2_{\hat{d}_j(t)}$ undergoes a process of adding the square of the new point residual and deleting the square of the old point residual based on its parameters, so the weight of each subset changes.

III. PERFORMANCE ANALYSIS

In this section, the time complexity of the proposed PRPS is first analyzed theoretically and compared with the state of the art. It is easy to figure out that time complexities of LS fitting can be evaluated as $O\left(k^3 + k^2n + kn^2\right)$, where k stands for the number of parameters and n stands for the number of fitting data [34]. Therefore, for RPS applied in this paper, the time complexities of fitting are $O\left(p\left(k^3 + k^2m + km^2\right)\right)$ and the time complexities of weighting average is $O\left(kpn + p\right)$, so the total time
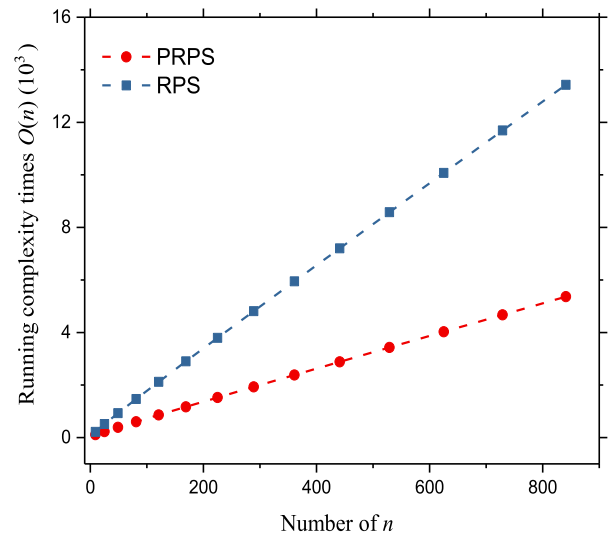

FIGURE 2. Time complexity comparison between the RPS and PRPS.

complexities of RPS is $O\left((k^3 + 1)n^{\frac{1}{2}} + k^2n + 2kn^{\frac{3}{2}}\right)$. The corresponding one of PRPS is $O\left(k^3 + (k^2 + 1)n^{\frac{1}{2}} + 2kn\right)$. Following the low-order ($k \leq 3$) polynomial assumption for fitting, the time complexities of RPS and PRPS are usually no more than $O\left(28n^{\frac{1}{2}} + 9n + 6n^{\frac{3}{2}}\right)$ and $O\left(27 + 10n^{\frac{1}{2}} + 6n\right)$, respectively. Fig.2 illustrates the theoretical trend of time complexities $O(n)$ of the above methods.
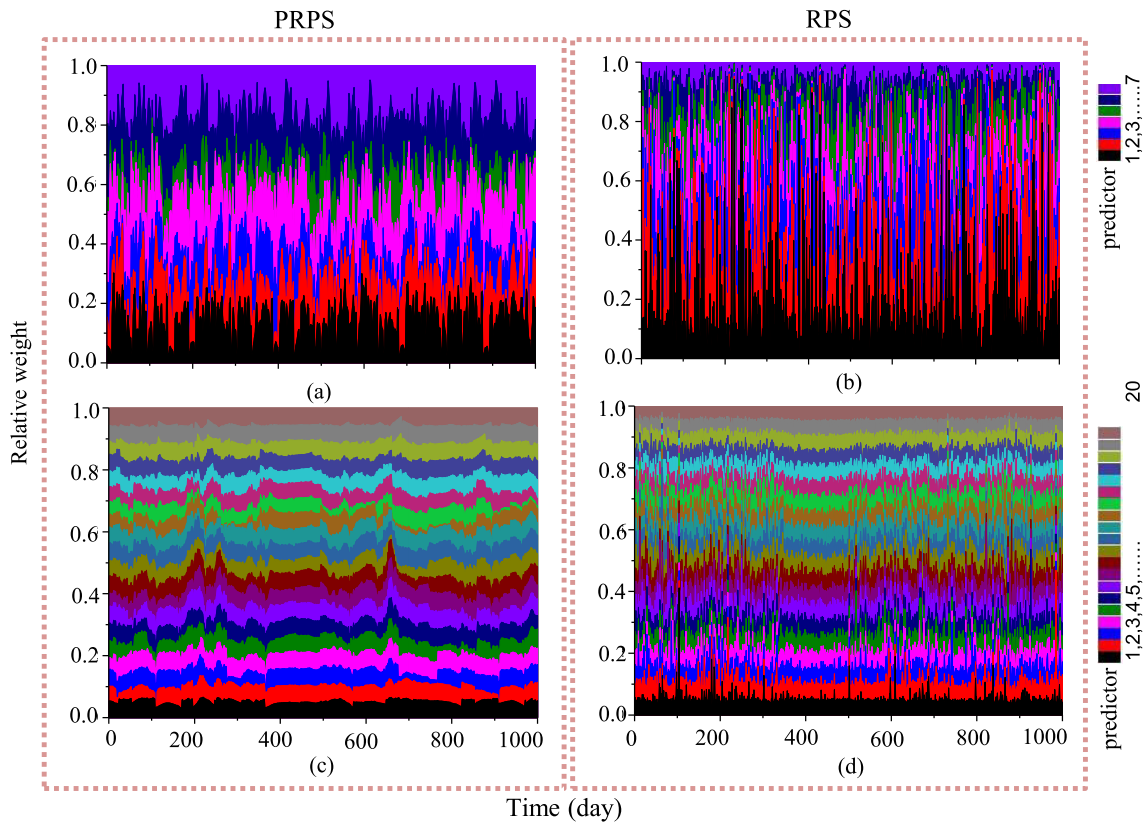
FIGURE 3. Weight distributions for PRPS and RPS on the number of subsets p=7 in (a) and (b), p=20 in (c) and (d).

A. SIMULATIONS

The simulation procedure with similar parameters [29] is used in this work. The frequency difference of an atomic clock relative to its reference is expressed as the formula:

$$y(t) = [a + \varepsilon_1 \cdot GN_1(\mu_1, \sigma_1)] + [b + \varepsilon_2 \cdot GN_2(\mu_2, \sigma_2)]t \quad (5)$$

where a and b represent the frequency and frequency drift respectively, $GN_1(\mu_1, \sigma_1)$ and $GN_2(\mu_2, \sigma_2)$ are defined as Gaussian noise with μ mean and σ variance ($\mu_1 = \mu_2 = 0$), ε_1 and ε_2 are the adjustable coefficients of Gaussian noise energy. The parameters used in the simulation are $a = \mu_1 = \mu_2 = 0, b = 10^{-15}, \varepsilon_1 = 1, \varepsilon_2 = 0.8, , \sigma_1 = 3 \times 10^{-30}, \sigma_2 = 4 \times 10^{-32}$.

According to the above simulation model, a simulated clock is applied to RPS and PRPS algorithms with the same parameters: the length of past data vector $Dn = 49$ and $n = 400$, the number of subsets $p = 7$ and $p = 20$, the length of each subset $m = 7$ and $m = 20$. As a comparison, the two algorithms are performed to predict 1000 times respectively. Fig.3 shows the weight distributions for two algorithms. Fig.3(a) and Fig.3(c) present the weight distributions of PRPS when $p = 7$ and $p = 20$ respectively whereas Fig.3(b) and Fig.3(d) show the weight distributions of RPS. Comparing Fig.3(a) with Fig.3(b) or Fig.3(c) with Fig.3(d), we can see
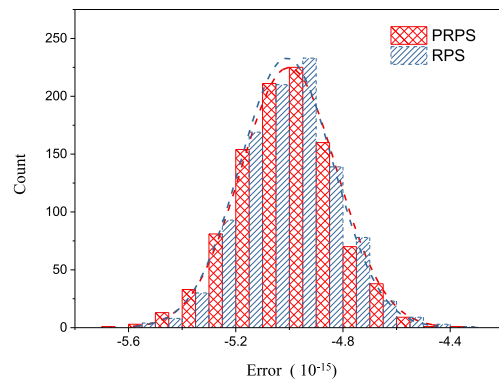

FIGURE 4. The errors' histogram with respect to prediction time t = 1 d.

that the weight of PRPS changes more smoothly under the same parameter setting due to pseudo random strategy. On the other hand, comparing Fig.3(a) with Fig.3(c) or Fig.3(b) with Fig.3(d), a larger number of subsets p in the same algorithm leads to a more stable weight distribution change for any two consecutive moments. It could be helpful to select appropriate parameters of RPS and PRPS to reduce the fluctuation of prediction values. Obviously, on the one hand, the larger subset sizes p means the bigger corresponding sampling window

size, and the bias estimated by one subset data to represent all data increases. On the other hand, the larger subset sizes p means more prediction values and a weighted average of all prediction values decreases the variance.

To confirm the predictability of the PRPS algorithm, 49 past data points of the simulated clock are firstly divided into 7 subsets. Then two algorithms were performed to predict 1000 consecutive data points. The distribution histogram of the prediction errors of RPS and PRPS algorithms is compared in Fig.4. At prediction time $t = 1\ d$, the prediction errors are normally distributed. The prediction errors are calculated by the difference of the predicted value and the measured value. Two fitting polynomials of the histograms are much related. As shown in Fig.5, the long-term prediction errors of two algorithms concerning the time from 1 day to 45 days increase gradually. The gray shadow is the standard deviation of real data at its corresponding time, the average prediction error of the two algorithms is both within the shadow. The unilateral prediction error also was influenced by its uncertainty. According to the error distribution in Fig.4, the prediction errors of two algorithms that are taken considered with the uncertainty are smaller than three times the real data standard deviations. Hence, PRPS and RPS show similar predictability.

The major time sinks of RPS and PRPS in the whole prediction process are random grouping and polynomial fitting, which depend on the number of subsets and the length of each subset. In the PRPS algorithm, different from RPS, random grouping is only performed once. In other words, only one in which needs to perform polynomial fitting due to replacing the data point at minimum index i with a new measured value. The 1000 predictions were performed with RPS and PRPS for the simulated clock according to (4). The running time comparison between the two algorithms is shown in Fig.6. With the increasing of subsets, both algorithms show a rise in running time, but PRPS shows an advantage for operational efficiency.
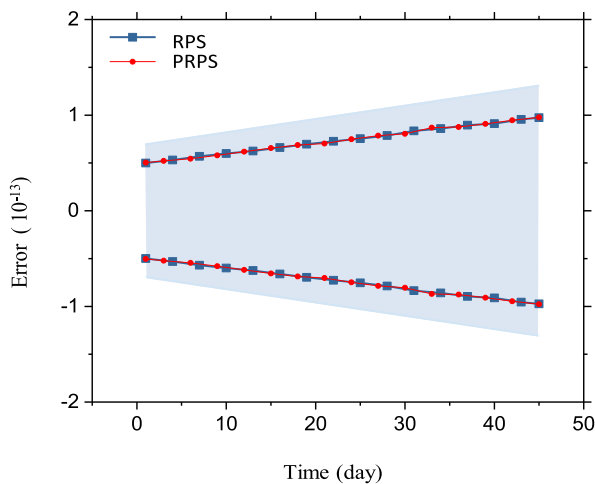

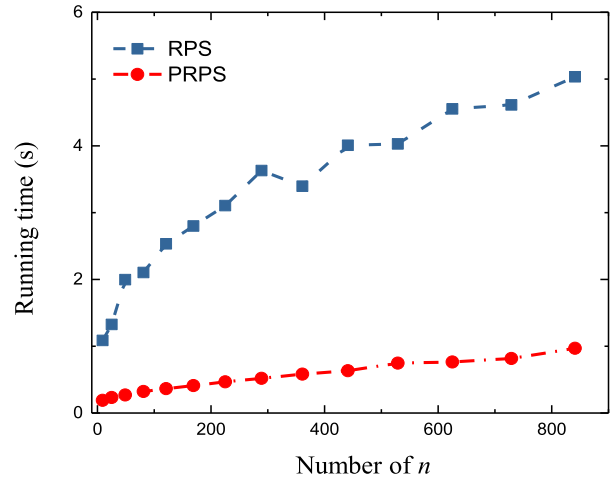**FIGURE 5.** Long-term predictability of RPS and PRPS.

FIGURE 6. Time consumption comparison between RPS and PRPS.

B. EXPERIMENTS

PRPS was applied to the cesium clock (Cs-clock) and hydrogen maser (H-maser), which are measured relative to UTC(NIM), the primary time and frequency standard of China. The predicted period of each clock was limited to 15 days. As shown in Fig. 7, the prediction uncertainty of two atomic clocks was investigated and the PRPS showed comparable predictability with RPS.

IV. DISCUSSION

In section III, the time complexity of the LS, RPS, and PRPS are compared, and the proposed PRPS is more efficient than the others. Although the Kalman filter approach is still the most efficient way for the clock real-time prediction and the theoretical time complexity of it is around $O(k^3)$, RPS and PRPS have their advantages mentioned in section II. Such as, for minor jumps [29], RPS may have a greater potential advantage than the Kalman filter to reduce prediction errors due to anomalous clock behavior.

For the real clock data, the running time of RPS and PRPS is not shown in part B of section III. There is no controversy that the running time of PRPS also decreases based on the theoretical and simulated studies mentioned in part A of section III. Further potential usage of PRPS is detecting anomalous behaviors from the continuously varying weights of predictors. In PRPS, the weight of the predictor shows a continuous change in Fig.3, therefore a sudden change in the weight of the same predictor may mean that the new data is a jump. RPS, on the other hand, must achieve the same purpose by comparing the weights of the predictors with each other. In other words, PRPS is also a more efficient way than RPS in terms of detecting anomalous behaviors.

PRPS is derived from RPS, but it does not fully inherit all of the properties of RPS, such as time translation invariance (homogeneity of time). In RPS, the siding window could be fixed time indexes, which means the fitting is applied in a fixed time interval T with changed sampling data. This
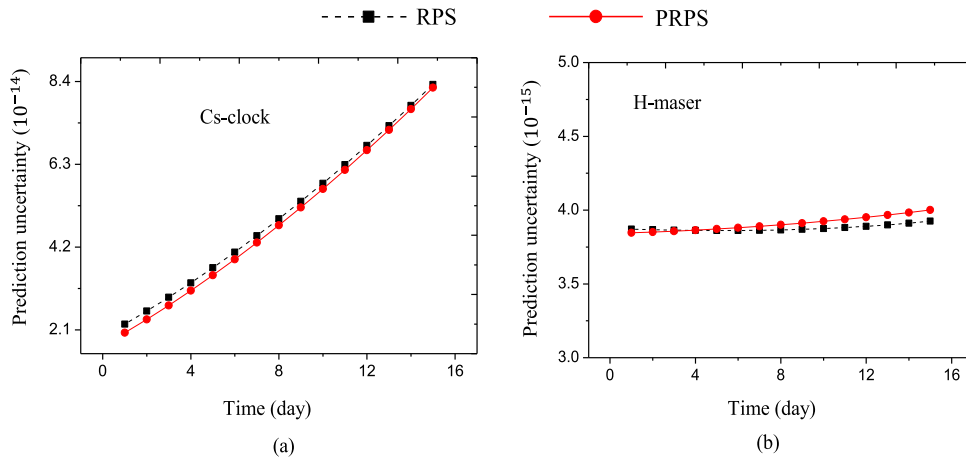
FIGURE 7. Prediction uncertainty of Cs-clock and at NIM.

makes the calculation of residuals and $u^2_{\hat{d}_j(t)}$ less susceptible to the measurement instant, so that weights calculated at each window are more sensitive to measurement data. It is clear in Fig.3 that the weights of RPS always fluctuate more strongly than the weights of PRPS at any fixed instant. However, this does not mean that RPS has significantly smaller prediction errors or prediction uncertainty than PRPS as shown in Fig.4, Fig.5, and Fig.7. The reason mainly comes from the calculation of weight ω_j is non-linear. Whereas the weights of predictors affected by jumps decrease, it necessarily results in the weights of other predictors rising. This relationship is not simply a linear increase on one side and a linear decrease on another side. The final prediction results are derived from the weighted average of all predictions, rather than focusing only on the worst-performing or the best-performing individual predictor. It remains a result of the trade-off of variance and bias for combined predictors. Indeed, for colored noises, we do not currently do an in-depth discussion of whether the method is effective, which is indeed what can be investigated further.

Although PRPS exhibits a lower time complexity than RPS, it requires more stability for the sampling of the clock data itself. Comparing PRPS to RPS, forgoing random grouping in a sliding window means that two or even more anomalous clock behaviors are more likely to be included within the same subset of data. This may cause bias in predictions and result in these jumps not being effectively identified. Therefore, the anomalies contained within the sliding window should be relatively low. In practice, the number of anomalies is best lower than p in the sliding window. This is relatively easy to satisfy for hydrogen or cesium clocks with good performance, but it is still a harsh requirement for some low-cost atomic clocks or optical clocks. Therefore, the choice of PRPS to replace RPS must consider specific engineering scenarios and experimental conditions.

V. CONCLUSION
In this paper, PRPS was designed and developed based on RPS. RPS improves the robustness of the prediction

system, but it has a low operation efficiency on the other hand. Due to the time complexity, it requires a high hardware cost to apply RPS to real-time clock prediction. PRPS simplifies the random grouping with pseudo random strategy and exhibits a similar performance in prediction accuracy and prediction uncertainty in simulated and real clocks data.

PRPS is faster, more efficient, and easier to employ when utilizing a clock predictor as the output of a system than RPS or LS. As a comparison, PRPS takes only $1/p$ fitting time consumption as long as RPS starts from the second prediction.

REFERENCES
[1] Y. Gao, X. Gao, A. Zhang, W. Wang, D. Ning, C. Wang, D. Li, X. Liu, N. Liu, P. Wang, M. Li, P. Lin, W. Chen, Y. Lin, and T. Li, "The generation of new TA(NIM), which is steered by a NIM4 caesium fountain clock," *Metrologia*, vol. 45, no. 6, pp. S34–S37, Dec. 2008.

[2] P. B. Whibberley, J. A. Davis, and S. L. Shemar, "Local representations of UTC in national laboratories," *Metrologia*, vol. 48, no. 4, pp. S154–S164, Jul. 2011.

[3] G. Panfilo, A. Harmegnies, and L. Tisserand, "A new weighting procedure for UTC," *Metrologia*, vol. 51, no. 3, pp. 285–292, Jun. 2014.

[4] G. Panfilo and F. Arias, "The coordinated universal time (UTC)," *Metrologia*, vol. 56, no. 4, Jun. 2019, Art. no. 042001.

[5] J. Levine, "Introduction to time and frequency metrology," *Rev. Sci. Instrum.*, vol. 70, no. 6, pp. 2567–2596, 1999.

[6] G. Panfilo, A. Harmegnies, and L. Tisserand, "A new prediction algorithm for the generation of international atomic time," *Metrologia*, vol. 49, no. 1, pp. 49–56, Nov. 2011.

[7] M. Y. Shin, C. Park, and S. J. Lee, "Atomic clock error modeling for GNSS software platform," in *Proc. IEEE/ION Position, Location Navigat. Symp.*, May 2008, pp. 71–76.

[8] C. Han, Y. Yang, and Z. Cai, "BeiDou navigation Satellite System and its time scales," *Metrologia*, vol. 48, no. 4, p. S213, 2011.

[9] E. D. Demaine, J. Lynch, and J. Sun, "An efficient reversible algorithm for linear regression," in *Proc. Int. Conf. Rebooting Comput. (ICRC)*, Nov. 2021, pp. 103–108.

[10] M. Reguzzoni, L. Rossi, C. I. De Gaetani, S. Caldera, and R. Barzaghi, "GNSS-based dam monitoring: The application of a statistical approach for time series analysis to a case study," *Appl. Sci.*, vol. 12, no. 19, p. 9981, Oct. 2022, doi: 10.3390/app12199981.

[11] F. Zhou, L. Zhao, L. Li, Y. Hu, X. Jiang, J. Yu, and G. Liang, "GNSS signal acquisition algorithm based on two-stage compression of code-frequency domain," *Appl. Sci.*, vol. 12, no. 12, p. 6255, Jun. 2022, doi: 10.3390/app12126255.

[12] Y. Liang, J. Xu, F. Li, and P. Jiang, "Nonlinear autoregressive model with exogenous input recurrent neural network to predict satellites' clock bias," *IEEE Access*, vol. 9, pp. 24416–24424, 2021.

[13] G. Panfilo and P. Tavella, "Atomic clock prediction based on stochastic differential equations," *Metrologia*, vol. 45, no. 6, pp. S108–S116, Dec. 2008.

[14] P. Tavella, "Statistical and mathematical tools for atomic clocks," *Metrologia*, vol. 45, no. 6, pp. S183–S192, Dec. 2008.

[15] Z. Li, K. Lee, R. N. Caballero, Y. Xu, L. Hao, M. Wang, and J. Wang, "Measuring clock jumps using pulsar timing," *Sci. China Phys., Mech. Astron.*, vol. 63, no. 1, Aug. 2019, Art. no. 219512.

[16] J. Azoubib, M. Granveaud, and B. Guinot, "Estimation of the scale unit duration of time scales," *Metrologia*, vol. 13, no. 3, pp. 87–93, Jul. 1977.

[17] P. Tavella and C. Thomas, "Comparative study of time scale algorithms," *Metrologia*, vol. 28, no. 2, pp. 57–63, Jan. 1991.

[18] Y. Wu, X. Zhu, Y. Huang, G. Sun, and G. Ou, "Uncertainty derivation and performance analyses of clock prediction based on mathematical model method," *IEEE Trans. Instrum. Meas.*, vol. 64, no. 10, pp. 2792–2801, Oct. 2015.

[19] L. Galleani and P. Tavella, "Robust detection of fast and slow frequency jumps of atomic clocks," *IEEE Trans. Ultrason., Ferroelectr., Freq. Control*, vol. 64, no. 2, pp. 475–485, Feb. 2017.

[20] L. Sobolewski and W. Miczulski, "Methods of time series preparation based on UTC and UTCr scales for predicting the [UTC-UTC(PL)]," *J. Phys., Conf. Ser.*, vol. 723, Jun. 2016, Art. no. 012040.

[21] J. M. López-Romero and N. Díaz-Muñoz, "Progress in the generation of the UTC(CNM) in terms of a virtual clock," *Metrologia*, vol. 45, no. 6, pp. S59–S65, Dec. 2008.

[22] H. Song, S. Dong, W. Wu, M. Jiang, and W. Wang, "Detecting an atomic clock frequency anomaly using an adaptive Kalman filter algorithm," *Metrologia*, vol. 55, no. 3, pp. 350–359, Apr. 2018.

[23] I. D. Leroux, N. Scharnhorst, S. Hannig, J. Kramer, L. Pelzer, M. Stepanova, and P. O. Schmidt, "On-line estimation of local oscillator noise and optimisation of servo parameters in atomic clocks," *Metrologia*, vol. 54, no. 3, pp. 307–321, Jun. 2017.

[24] W. Miczulski and Ł. Sobolewski, "Algorithm for predicting [UTC–UTC(k)] by means of neural networks," *IEEE Trans. Instrum. Meas.*, vol. 66, no. 8, pp. 2136–2142, Aug. 2017.

[25] J. A. Davis, S. L. Shemar, and P. B. Whibberley, "A Kalman filter UTC(k) prediction and steering algorithm," in *Proc. Joint Conf. IEEE Int. Freq. Control Eur. Freq. Time Forum (FCS)*, May 2011, pp. 1–6.

[26] L. Galleani, "A tutorial on the two-state model of the atomic clock noise," *Metrologia*, vol. 45, no. 6, pp. S175–S182, Dec. 2008.

[27] C. Zucca and P. Tavella, "A mathematical model for the atomic clock error in case of jumps," *Metrologia*, vol. 52, no. 4, pp. 514–521, Aug. 2015.

[28] C. Zucca, P. Tavella, and G. Peskir, "Detecting atomic clock frequency trends using an optimal stopping method," *Metrologia*, vol. 53, no. 3, pp. S89–S95, Jun. 2016.

[29] Y. Wang, Y. Chen, Y. Gao, Q. Xu, and A. Zhang, "Atomic clock prediction algorithm: Random pursuit strategy," *Metrologia*, vol. 54, no. 3, pp. 381–389, Jun. 2017.

[30] Y. Wang, A. Zhang, Y. Gao, Q. Xu, and Y. Lin, "Uncertainty analysis of clock prediction based on a random pursuit strategy," *Meas. Sci. Technol.*, vol. 29, no. 7, Jul. 2018, Art. no. 075015.

[31] P. Bühlmann and B. Yu, "Analyzing bagging," *Ann. Statist.*, vol. 30, no. 4, pp. 927–961, 2001.

[32] P. Bühlmann, "Bagging, subagging and bragging for improving some prediction algorithms," in *Recent Advances and Trends in Nonparametric Statistics*, M. G. Akritas and D. N. Politis, Eds. Amsterdam, The Netherlands: JAI, 2003, pp. 19–34.

[33] P. Ma, M. Mahoney, and B. Yu, "A statistical perspective on algorithmic leveraging," in *Proc. Int. Conf. Mach. Learn.*, Jan. 2014, pp. 91–99. [Online]. Available: https://proceedings.mlr.press/v32/ma14.html

[34] L. Galleani and P. Tavella, "On the use of the Kalman filter in timescales," *Metrologia*, vol. 40, no. 3, pp. S326–S334, Jun. 2003.

[35] C. A. Greenhall, "A Kalman filter clock ensemble algorithm that admits measurement noise: Corrections and update," *Metrologia*, vol. 44, no. 6, pp. 491–494, Nov. 2007.

[36] C. A. Greenhall, "A review of reduced Kalman filters for clock ensembles," *IEEE Trans. Ultrason., Ferroelectr., Freq. Control*, vol. 59, no. 3, pp. 491–496, Mar. 2012.

[37] M. Suess and C. A. Greenhall, "Combined covariance reductions for Kalman filter composite clocks," *Metrologia*, vol. 49, no. 4, pp. 588–596, Aug. 2012.

[38] T. K. Ho, "The random subspace method for constructing decision forests," *IEEE Trans. Pattern Anal. Mach. Intell.*, vol. 20, no. 8, pp. 832–844, Aug. 1998.

QIAN XU received the Ph.D. degree from the Beijing Institute of Technology, China, in 2021. She is currently a Postdoctoral Researcher with the Time and Frequency Division, National Institute of Metrology (NIM), China. Her major research interests include the atomic clock prediction algorithm and technology of timekeeping.

YU CHEN received the master's degree from the Beijing Institute of Technology, in 2013. After graduation, he worked as an Engineer with the Shaanxi Cancer Hospital for two years. Since 2015, he has been working with China National Intellectual Property Administration (CNIPA) as a Patent Officer. His current research interests include patent retrieval modeling, time scale algorithm, and biomedical image and signal processing.

YUZHUO WANG received the Ph.D. degree from the Beijing Institute of Technology, in 2015. Since then, he has been with the Time and Frequency Division, National Institute of Metrology (NIM). His current research interests include time scale algorithm and precise measurement about time and frequency.

YUAN GAO received the bachelor's degree from the University of Electronic Science and Technology, China, in 1996, and the master's degree from the Beijing University of Technology, in 2010. Since 1996, he has been working with the Time and Frequency Division, National Institute of Metrology (NIM). He became a Research Fellow, in 2018. His research interest includes the national primary standard for time. He has received the First and Third Class Prizes of the National Science and Technology Progress Award.

AIMIN ZHANG received the B.S. degree from Peking University, in 1987, and the M.S. degree from the National Institute of Metrology (NIM), in 1990. Since then, she has been working with the Time and Frequency Division, NIM. She is in charge of the generation and maintenance of UTC (NIM), which is the time and frequency primary standard in China. She is currently the APMP TCTF Chair.

●●●